Fluid Inclusion Characteristic of Tin-Tungsten and Copper Mineralisation in Tosham Igneous Complex of North Delhi Fold Belt, North-Western India

Girish Kumar M.[1,*], Nevin, C. G.[1], Madhushree Mondal[2], Abhishek Anand,[3]
R. P. Nagar[4], and Subhaish Ghosh[1]

[1]National Centre of Excellence in Geosciencences Research, Bangalore, India.
[2] NCEGR, Geological Survey of India.
[3] Petrology Division, WRO, Geological Survey of India, India.
[4] Deputy Director General, India.
*Correspondence: girishgeosu@gmail.com (G.K.M.)

Abstract—**Tosham igneous complex occurs along northern part of the middle Proterozoic North Delhi fold Belt and metasediments of Delhi Supergroup. It comprises of Tosham porphyritic granite, rhyolite and quartz-porphyry. The Tosham granite and rhyolite hosts the tin-tungsten and copper mineralisation. Cassiterite and Wolframite occurs within the quartz veins and associated with other ore minerals such as chalcopyrite, pyrrhotite and pyrite. The foliation trend of the metasediments is N20° to 40°E parallel to the long axis of the hill. The mineralisation occurs near the granite-metasediments or granite-rhyolite contact in the western and eastern mineralised zones within Tosham hill. EPMA studies confirm the presence of cassiterite, pyrite, chalcopyrite, pyrrhotite, sphalerite etc. The fluid inclusions study reveals the existence of aqueous-gaseous (H_2O-CO_2+NaCl) fluid that underwent phase separation and gave rise to gaseous (CO_2) inclusion. The carbonic inclusions show depression in $Tmco_2$ (-65.2°C) due to the presence CH_4 with CO_2 and also large no. of CH_4 inclusions are present and were confirmed by Raman spectroscopy and it was first time reporting in this area. The abundant of CH_4 inclusions over the CO_2 inclusions considered to be one of the diagnostic features of reduced porphyry copper type deposits. The salinity of tin/ tungsten mineralisation shows high to low (1.9 to 42.68 wt % NaCl equivalents) and trapped at the estimate PT range from 2.1 to 3.5 kbar and 310 to 460°C. The eutectic temperature (Te) ranges from -50°C to -30°C reveals that the presence of chloride complexes such as $FeCl_2$/$MgCl_2$ and $CaCl_2$ indicating the involvement of brines or complicated chloride mixtures in transporting Sn-W to the fluid system and evaluation of Sn-W ore fluids by high-salinity and high-temperature with the magmatic-hydrothermal activity either by immiscibility or mixing of fluids and evolution of granite/rhyolite induced the fluidisation and the presence of CH_4/CO_2 influx might have triggered precipitation Sn-W and Cu mineralisation in the area.**

Keywords—**tosham, wolframite, tin, copper, granite, fluid inclusion**

I. INTRODUCTION

The middle Proterozoic Delhi Fold Belt of western India hosts important base metal mineralisations in the entire stretch from southern part of Rajasthan to northern continuity in Haryana. In the northern part, mainly the Tosham area, comprised of Cu and Sn-W mineralisation. McMohan (1886) Ref. [1], first described the geology of the area and studied the petrography of felsites, quartz-porphyry, granite and other rock types of this area and correlated the felsic volcanics and granites of Tosham with the Malani suite of igneous rocks of western Rajasthan. Kochhar (1983) Ref. [2] established a close association in space and time between the explosive felsic lava and high level nonorogenic subvolcanic granite which form distinct ring structure and also suggested that a hot spot related tectonics responsible for the igneous activity at Tosham. Rajashekharappa (1983) Ref. [3] gave petrographic studies and major elements data of all the rock types of the area and suggested the structure of Tosham igneous complex represents a caludron subsidence of a graben type.

Awasthi *et al*., (1977) Ref. [4] reported the occurrence of copper mineralization from this area and emphasised on the need for exploration for copper mineralization, whereas Dey (1978) Ref. [5] recorded the occurrence of copper minerals such as malachite, azurite, cuprite and chalcopyrite and concluded that copper mineralization is mainly restricted to western flanks of Tosham hillock. Geological Survey of India has carried out exploration for base metals involving geological mapping, geochemical sampling and drilling operations was carried out in and around Tosham area (Choudhary et. al. 1984 and Kochhar *et al*., 1985) Ref. [6, 7]. Somani (2006) Ref. [8] studied fluid inclusions of hydrothermal solutions associated with Tin-Tungsten and copper mineralization at Tosham. Murao et al. (2008) Ref. [9] has carried out mineralogical evolution of Indium at Tosham in comparison with Goka area of Japan. Baniranjan Mishra and Surabhi Srivastava (2018) Ref. [10] carried out exploratory drilling in the

northern extension of Tosham hill for the understanding mineralisation in the northern extension of Tosham hill.

Fluid inclusions in transparent gangue minerals are thus commonly used to investigate metal precipitation conditions. This assumption is mainly based on the close spatial association of gangue and ore minerals (Campbell et al., 1984) Ref. [11]. In the last decade, new data sets have been published on the characterization of the fluid systems present during ore formation in different tin-tungsten and polymetalic deposits worldwide, including advanced studies of Raman spectroscopy.

The present study deals with the geological setting of tin-tungsten and copper mineralisation hosted by granite/rhyolite in Tosham igneous complex. The petrographic and EPMA studies confirm that cassiterite occurs as disseminated and it is associated with pyrrhotite and chalcopyrite. The fluid inclusion studies of quartz veins reveals the evaluation of ore forming fluids for understanding of genesis and formation mechanism of Sn-W-Cu mineralization associated with the igneous complex of Tosham.
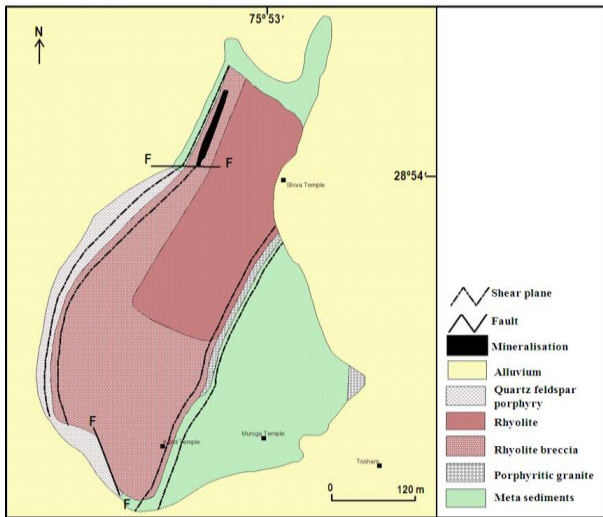

Figure 1. Geological map of the Tosham area (Modified after Kochar, 1983).

Figure 2a. Field photographs of rhyolite.

Figure 2b. Field photographs of porphyritic granite.

Figure 2b. Field photographs of porphyritic granite.

Figure 2d. Field photographs of meta sedimentary.

II. GENERAL GEOLOGY

The Tosham igneous complex comprises of granite porphyry and rhyolite are intruded in metasediments of Delhi Super Group of Proterozoic age and are equivalent to the Malani suite of rocks represented by the rhyolites and granites. The exposures of granite and rhyolite occur in isolated patches in a vast stretch of aeolin sands. The dome shaped Tosham hill forms a prominent topographic high above the plains. The three main suits of rocks were identified in the area are: quartz feldspar porphyry, central mass of rhyolites forming steep vertical cliff and also covered by rhyolite breccia, porphyritic granite and metasediments. The porphyritic granite intrudes metasediments and subsequently, both these formations have been intruded by hypabyssal rhyolite which forms the core/central part and surrounded by the rhyolite breccia of the Tosham hill. The foliation trend of the

metasediments is N20 to 40E parallel to the long axis of the hill. Two prominent shear zones trending NNE and NNW with sub-vertical attitude, occur on the western and eastern faces of Tosham hill (Fig. 1). They are 5-10m wide and marked by close spaced open fractures with replacement of sulphides by iron oxides and malachite stains.

The Tosham area consists of granite and rhyolite surrounded by sand and alluvium. Tosham igneous complex rocks of granite and rhyolite are related to Erinpura-Malani plutonic-volcanic Neoproterozoic acid magmatic event. The isolated hillocks of Tosham exposed are mainly of Post Delhi granitoids and consists of rhyolite in the central part of the complex showing sharp contacts with rhyolite breccia and porphyritic granite. Murao et al. (2008) Ref. [09] suggested that the granites and rhyolites in the Tosham region formed at ~800 Ma, rhyolite effusion being slightly later than granite emplacement. This is also clearly borne out by the relationship between the two rock types seen in transverse sections across the Tosham hill. It is variegated from grey to yellowish grey to various shades of purplish brown (Fig. 2a). Flow banding is inward at high angles indicating magma viscosity high enough to prevent significant extrusion from the central part (Gupta and Rajashekharappa, 1983) Ref. [12]. Rhyolite breccia occurs along the margins of the rhyolite and granite porphyry. The rhyolite breccia contains blocks of both accessory and accidental types of various rocks of volcanic matrix. Kochhar (1983) Ref. [2] has identified the rhyolite breccia on the basis of the sub-angular to angular and sub-rounded to rounded fragments of granite porphyry. The porphyritic granite exposed in the south-western slope of the Tosham hill and the continuity of this rock type is concealed due to aeoline cover (Fig. 2b). The Quartz feldspar porphyry dykes were observed in the field one is at SE side of the hill and another is NE side of the hill. This is clearly cutting across the rhyolite (Fig.2c) and at contact chilled margins and size reduction is noticed. Meta sedimentary rocks of Delhi super group of rocks observed in the eastern side and NE of the Tosham hill and it mainly consist of quartzite, micaceous quartzite, andalusite bearing quartzite and schists (Fig.2d). The quartzite is dull white to light brown colour and medium grained and at many places, massive iron oxide staining observed. Two major shear zones on the western and eastern side of the rhyolite hills of Tosham are associated with mineralization. The surface indications like sulphide leaching, gossans, malachite stains and old working are the main evidence of mineralization. Tosham hill contains numerous joint sets filled with iron oxide minerals and at places fresh sulfide is also noticed.

III. PETROGRAPHY

Meta sedimentary rocks of Delhi super group of rocks observed in the eastern side and NE of the Tosham hill. Metasedimentory rocks shows fine to medium grained quartz, muscovite, sericite, iron oxide and opaque minerals are common. Crude foliation planes define by micaceous minerals seen at places. Quartz grain

boundaries are sutured, interlocking with undulose extinction. Iron oxide is seen as patches throughout the sections (Fig. 3a). The granite is porphyritic in nature and consists of pinkish to light greyish at places coarse grained K-feldspar and quartz grains set in a medium grained groundmass of quartz, feldspar, biotite and muscovite and minor amount of the zircon, apatite and iron oxide. The rock is highly altered and the feldspar grains shows greenish colour and at places altered to micaceous minerals (Fig. 3b). The rhyolite rock is very fine grained, compact and massive. It is variegated colours of greenish grey, pinkish and brownish. The outcrop contains many joints filled with iron oxide and sulfides. The leaching of the iron oxide may be the reason for the different colour to this rock. Rhyolitic tuff consists of quartz embedded in a very fine grained matrix showing a holocrystalline texture. The fine grained matrixes are orthoclase feldspar, biotite and muscovite mica (Fig. 3c).
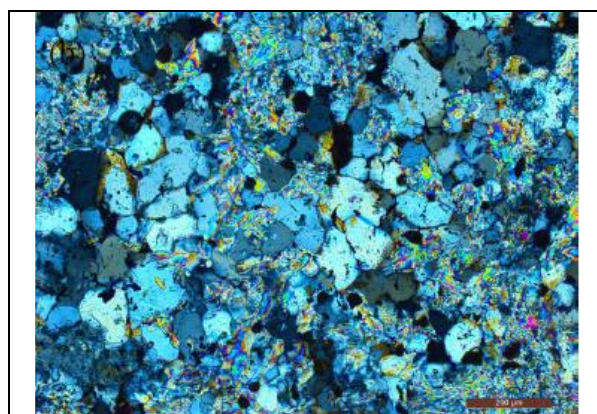

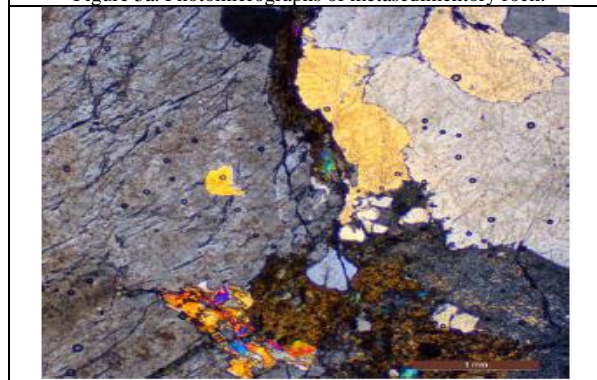Figure 3a. Photomicrographs of metasedimentory rock.

Figure 3b. Photomicrographs of porphyritic granite.

Figure 3c. Photomicrographs of rhyolite with porphyry clasts of quartz embedded in fine grained matrix.

Ore microscopic studies were carried out on samples collected from surface and sub surface from Tosham area. The samples collected from the mineralized zone from the borehole drilled north of Tosham hill have studied (Fig. 3d & e). The major ore minerals observed under microscope are cassiterite, pyrrhotite, chalcopyrite and pyrite. Cassiterite usually seen associated with silicate minerals and sometimes seen associated with pyrrhotite and chalcopyrite and at fracture planes pyrrhotite and chalcopyrite is seen intruded into the grain boundaries of cassiterite (Fig. 3f). The pyrite is seen as fracture filled in later stage (Fig. 3g).

Figure 3d. Drill core of chalcopyrite mineralized zone.

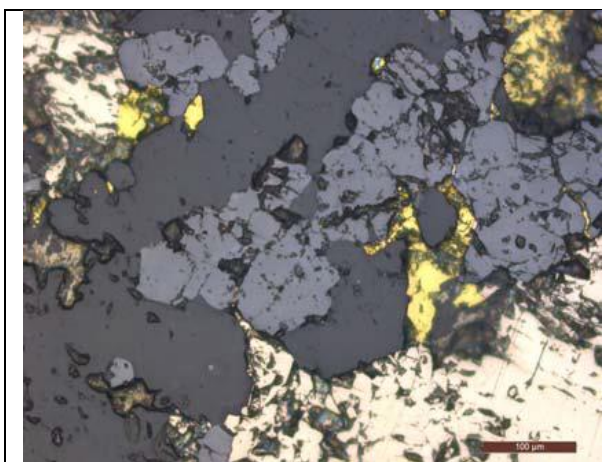Figure 3e. sulphides seen as disseminations.

Figure 3f. Pyrrhotite and chalcopyrite seen intruded into the grain boundaries of cassiterite.
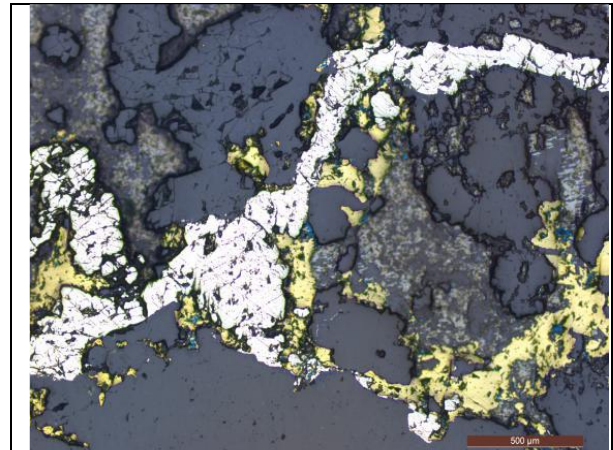

Figure 3g. Pyrite seen associated with chalcopyrite as a fracture filling.

IV. SN-W-CU MINERALISATION

Tosham igneous suite comprising of granite and rhyolite hosts the tin-tungsten and copper and are associated with sulphide mineralisation localised mostly along the western and northern part of the Tosham igneous complex. An old working is located at western side at the contact of rhyolite and porphyritic granite. At western side of Tosham hill, malachite is seen associated with iron oxide veins and at places yellowish and red coloured gossans associated with iron oxides and at places hematite ore associated with quartz veins and even seen filled in joints and fractures. The main ore of tin (cassiterite) occurs as minute grains, specks, blades and disseminations in contact between meta sedimentary rock with porphyritic granite. The other associated ore minerals include wolframite, chalcopyrite, pyrite, stannite, pyrrhotite, cubanite, covellite etc. Cassiterite and Wolframite occurs intimately associated with quartz veins as fine 0.02 mm to coarse 1 cm grain and intergrowth with gangues as well as sulphides mainly chalcopyrite. It also occurs as exsolved belbs within chalcopyrite. The Mineral zonality is observed from the relative variations in the contents of tin, tungsten and copper. The bulk of mineralisation occurs at near the granite-metasediments or granite-rhyolite contact in the western and eastern mineralised zones within the Tosham hill. Copper mineralisation occurs in the forms of malachite and azurite stains, cuprite and chalcopyrite with pyrite, sphalerite along the contact zone of central rhyolite and western granite porphyry as fracture filling and disseminations, where as pyrite occurs as a thin stringers and veinlets and the tin mineralisation is associated with copper and tungsten. It averages 0.16% W, 0.53% Cu and 0.429% Sn and estimated 5.10 million tonnes (MECL). Based on detailed regional exploration of GSI, ore reserves of Sn, W and Cu have been estimated at 2.23 million tonnes up to a depth of 237 m below MSL with average grade of 0.28% Sn, 0.18% W and 0.24% Cu (Wokhoo and Prasad, 1989) Ref. [13].

V. EPMA STUDIES

Chemical compositions of the ore polished thin sections were analyzed with the help of four-wavelength dispersive spectrometer (WDS) attached to CAMECA SX-100 electron microprobe analyzer at Center of Excellence in Geosciences Research (NCEGR), Geological Survey of India (GSI), Bangalore. Acceleration voltage of 15 kV and 20nA beam current with a beam diameter of 1 μm. The counting time was 10 and 5 s for the peaks and the background, respectively. Calibration processes were carried out separately for both silicate and sulfide minerals by using appropriate natural standards were chosen for calibration and ZAF corrections were made by the program PAP (Pouchou and Pichoir, 1984) Ref. [14].

The EPMA analysis of ore mineralised veins sample from Tosham area shows presence of cassiterite, pyrite, chalcopyrite, pyrrhotite, sphalerite etc. The main ore mineral of Cassiterite is associated with pyrrhotite and chalcopyrite (Fig. 3h). Cassiterite also occurs as disseminated and large grains having an inclusion of chalcopyrite (Fig. 3i).
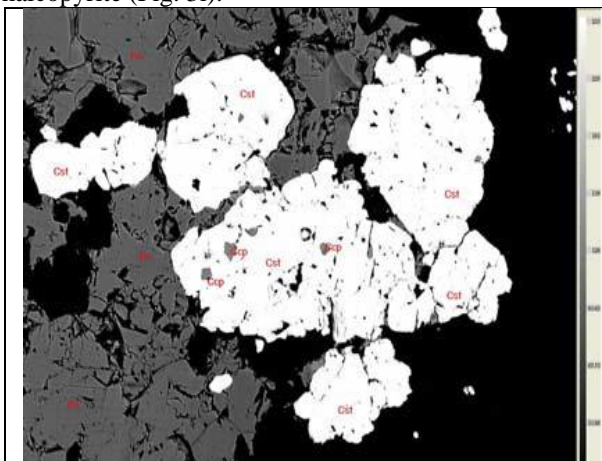

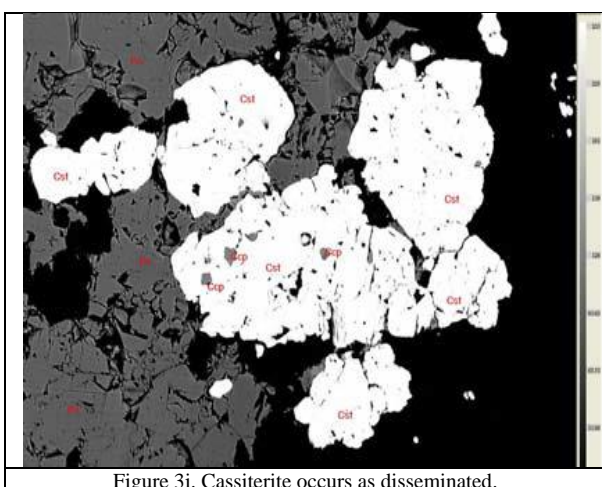Figure 3h. Cassiterite associated with chalcopyrite.

Figure 3i. Cassiterite occurs as disseminated.
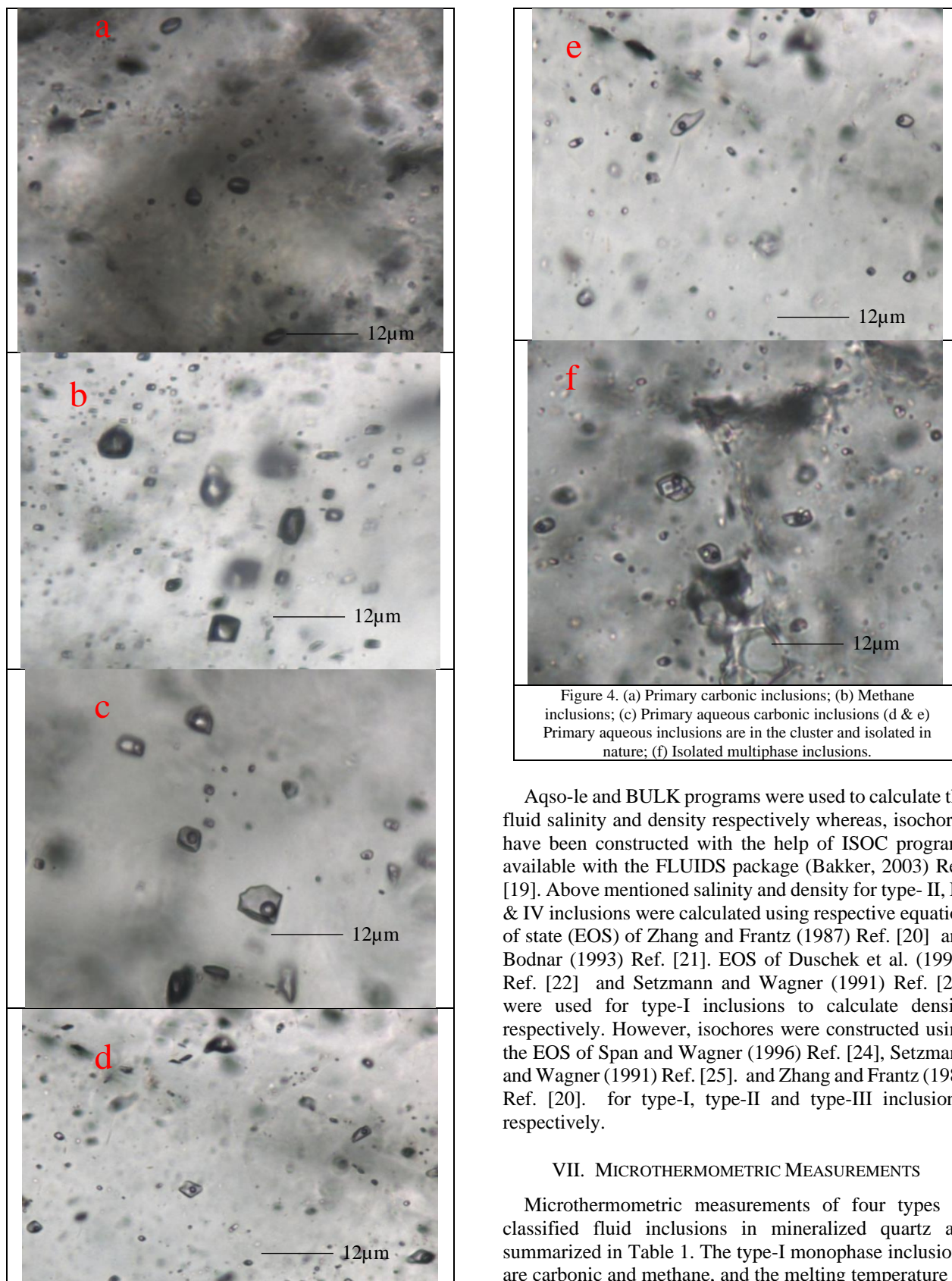
VI. FLUID INCLUSION STUDIES

Fluid inclusion parameters in the mineralized quartz veins associated with porphyritic granite and rhyolite sample were prepared doubly polished thin wafers (thickness ~ 0.3 mm). Fluid inclusion microthermometry was conducted with the help of a Linkam MDSG600 Heating and Freezing Stage attached with Olympus BX-50 petrological microscope at National Center of Excellence in Geosciences Research (NCEGR), Geological Survey of India (GSI), Bangalore. The stage can operate in a temperature range of −198 to 600°C. Proper periodic calibration of the stage was done using the pure H_2O-CO_2 synthetic standard inclusions obtained from Linkam.

Fluid Inclusion petrography studies were carried out for the identification of inclusions on the basis of genetic and phase types. The fluid inclusions were identified and broadly grouped them and classify in accordance with the classification principles and techniques outlined by Roedder (1984) Ref. [15] and Lu *et al.* (2004) Ref. [16]. In addition, abundance of fluid inclusions was noted following the methods of Touret (2001) Ref. [17]. An attempt was made in the light of new experimental studies by Bodnar et al. (1989) Ref. [18], on the morphology of fluid inclusions to correlate the different textural features of fluid inclusions with equilibration path. The size of the inclusions varies from 1.90 to 58.00μm. The size of vapour phase of water vapour/CO_2 bubbles varies from 0.39 to 5.50μm. Based on the phases present, they are grouped into four types: type-I inclusions are monophase carbonic or methane inclusions (type-IA primary monophase carbonic and type-IB methane inclusions), type-II primary aqueous carbonic inclusions and type-III primary aqueous bi-phase inclusions. Type-IV multiphase inclusions contain the halite crystal with cubes in nature.

The type-IA inclusions are monophase carbonic inclusions are occur as clusters/isolated and contains only one phase contain and some are two phases at room temperature (Fig. 4a). The CO_2 vapour is perfectly circular, spherical and is homogenized into the liquid phase. The type-1B inclusions are monophase methane inclusions and are occur as clusters/isolated and contains only one phase at room temperature (Fig. 4b) and these methane inclusions are reported first time in this area.

The type-II inclusions are less abundant and not so common, these inclusions occur in isolated pattern and contain CO_2 (liquid)-CO_2 (gas)-H_2O(liquid) (Fig. 4c). Type-III inclusions are comparatively more abundant than any other inclusions and these inclusions occur as isolated/clustered. (Fig. 4d & e). They are generally small and rounded as well as irregular and contain biphase H_2O-NaCl inclusions, that is homogenized to liquid upon heating. The proportion of the vapour phase is typically about 10% to 15% by volume. The type-IV inclusions contain aqueous liquid, and vapour and one more solids. The liquid to vapour ratios are similar to those in type-III inclusions. The solids are very small in size and anistropic and generally have high birefringence, although some solids are weakly birefringent or non birefringent (Fig. 4f).

Figure 4. (a) Primary carbonic inclusions; (b) Methane inclusions; (c) Primary aqueous carbonic inclusions (d & e) Primary aqueous inclusions are in the cluster and isolated in nature; (f) Isolated multiphase inclusions.

Aqso-le and BULK programs were used to calculate the fluid salinity and density respectively whereas, isochores have been constructed with the help of ISOC program, available with the FLUIDS package (Bakker, 2003) Ref. [19]. Above mentioned salinity and density for type- II, III & IV inclusions were calculated using respective equation of state (EOS) of Zhang and Frantz (1987) Ref. [20] and Bodnar (1993) Ref. [21]. EOS of Duschek et al. (1990) Ref. [22] and Setzmann and Wagner (1991) Ref. [23] were used for type-I inclusions to calculate density respectively. However, isochores were constructed using the EOS of Span and Wagner (1996) Ref. [24], Setzmann and Wagner (1991) Ref. [25]. and Zhang and Frantz (1987) Ref. [20]. for type-I, type-II and type-III inclusions, respectively.

VII. MICROTHERMOMETRIC MEASUREMENTS

Microthermometric measurements of four types of classified fluid inclusions in mineralized quartz are summarized in Table 1. The type-I monophase inclusions are carbonic and methane, and the melting temperature of methane was at lower temperature and it was confirmed by the Raman spectroscopy (Fig. 5).
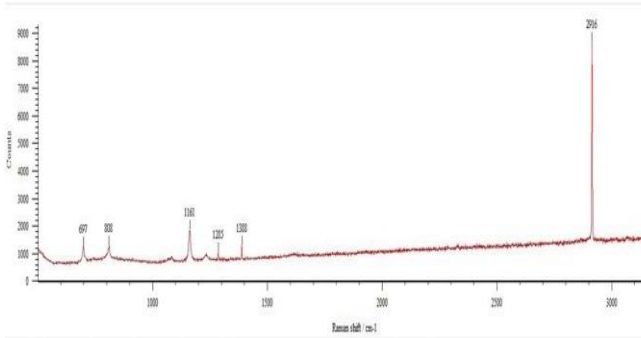
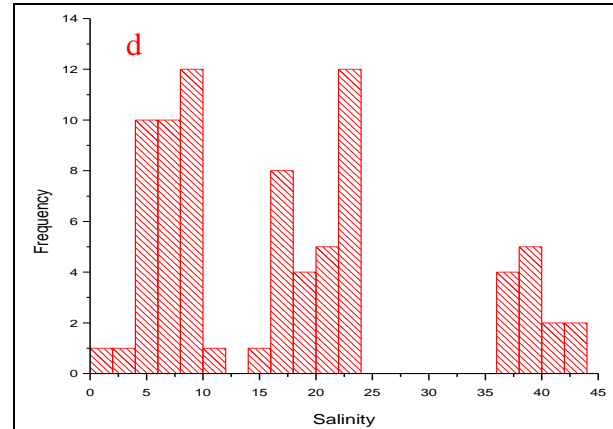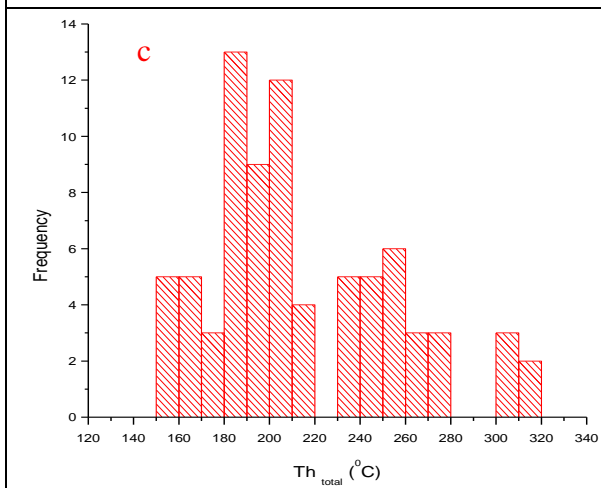Figure 5. CO2 and CH4 peaks detected in the primary monophase fluid inclusion from Tosham area.
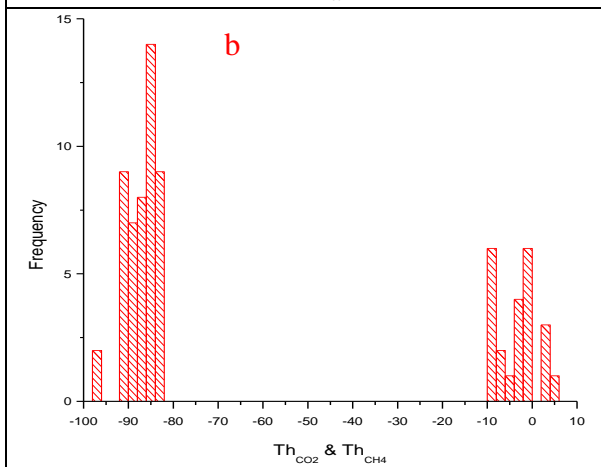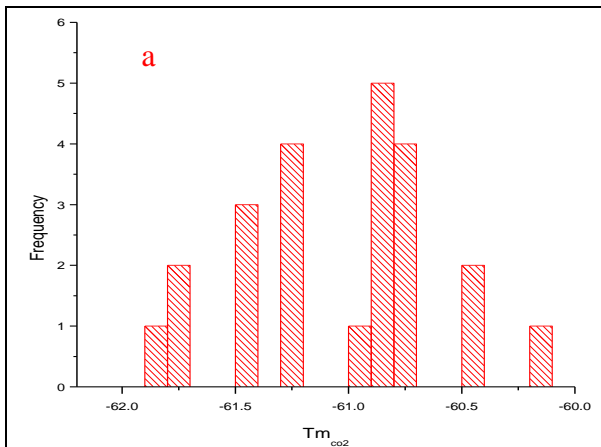

Figure 6. Histograms of the (a) Tm_{CO2}, (b) $Th_{CO2,ch4}$ (c) Th_{total} and (d) salinity in mineralised quartz veins.

The type-IA inclusions are primary carbonic inclusions formed solid CO_2 upon cooling. The solid CO_2 melt at the temperature between -61.9°C and -60.1°C. In most of the inclusions and in few inclusions the melting temperature observed at lower temperature is -60.5°C, -61.2 °C, -61.5 °C and -61.9°C. This lowering of melting temperature of CO_2 indicating admixtures of other gases such as CH_4/N_2 (van den Kerkhof, 1988; Brown and Lamb, 1989) Ref. [26, 27]. The melting temperatures (Tm_{CO2}) are graphically illustrated in histogram Fig. 6a. The temperature of homogenized of CO_2 into vapour phase at temperature -9.0 to 4.0 °C (density varies 0.90 to 0.97 g/cm3), which are graphically plotted in histogram Fig. 6b. The type-IA monophase methane inclusions melting temperature (Tm_{CH4}) was not possible to measure and only CH4 melting temperature (Th_{CH4}) was measured and varies between -97.0°C to -82.7°C (density varies 0.18 to 0.29 g/cm3) which are graphically plotted in histogram (Fig. 6b).

The primary aqueous carbonic inclusions (Type-II), inclusions are characterized by the nucleation of a vapour bubble on cooling, consistent with the composition of CO2(liquid)+CO2(gas)+H2O(liquid) +NaCl. These inclusions are coexisting with aqueous rich inclusions, suggesting that the fluid immiscibility might have occurred towards the stage of crystallization (Roedder, 1984) Ref. [15]. The range of homogenization temperature varies from 250 to 310 °C. The initial ice melting eutectic temperatures (Te) range from -32 to -50 °C with an average of -40.76 °C and this suggests that the major component in aqueous phase is NaCl±FeCl2 in the fluid system (Shepherd et. al., 1985) Ref. [28]. The final melting temperature of ice ranges from -3.9 to -7.2 °C (average -5.94 °C) corresponding with salinities of 6.22 wt.% to 10.73 wt.% NaCl eq. (average 9.07 wt.% NaCl eq.) following the equations of Bodnar (1993) Ref. [21]. The melting temperature of the CO_2 (Tm_{CO2}) ranges from -58.8 to -61.5°C and the homogenization temperature of CO_2 ranges from 16 to 26°C.The CO_2 density of aqueous carbonic inclusion varies from 0.73 to 0.88 g/cm³.

The type-III inclusions are aqueous inclusions and are frozen at temperatures mainly between -58 to -75 °C. The range of homogenization temperature varies from 158 to

245 ℃ (Fig.6c) and during the heating runs the first melting (eutectic) temperature (Teu) has been observed, ranging from -46.8 to -30 ℃ with an average of -39.61 ℃ and suggesting that the major component in aqueous phase is $MgCl_2±FeCl_2$ in the fluid system. The maximum eutectic temperature -46.8 ℃ may indicate the presence of $FeCl_2± MgCl_2$ with NaCl and H_2O (Shepherd et. al., 1985) Ref. [28]. The final melting temperature of ice (Tm_{ice}) ranges from -1.2 to -20.9 ℃ corresponding salinities of 1.97 to 22.98 wt.% NaCl equivalent. (Fig. 6d). The density of aqueous phase varies from 0.86 to 1.05 g/cm³. The type-IV inclusions are the aqueous multiphase inclusions contain aqueous liquid, a vapour bubble and a halite crystal and these halite crystals show characteristic feature of cubic outline. The size of the halite crystals varies from 1.5 to 9 µm (in terms of the largest edge) and 2.3 to 6 µm (diameter), respectively. The homogenization temperature of phase varies from 158 to 271℃ and total homogenisation temperature ranges from 289 to 353 ℃. The solid halite crystals melt at very high temperature at 353 ℃, this may due to they are accidentental trapping and are insignificant in numbers. The salinity ranges from 37.0 to 42.68 wt.% NaCl eq.

VIII.   DISCUSSIONS AND CONCLUSION

Tosham igneous complex are related to the Neoproterozic acid magmatic event. The anorogenic magmatism of Tosham is attributed to hot spot activity and is due to thermal processes in the asthenosphere (Kochhar, 1992) Ref. [2]. The Tosham igneous magmatism was triggered by mantle plumes and the release of volatiles from the magma, the melt becomes viscous and during the continued advance to higher level it crystallizes as rhyolite. The mineralisation of Sn-W and Cu in the western side of the contact between rhyolite and porphyritic granite. The main ore of tin (cassiterite) occurs as minute grains, specks, blades and disseminations in contact between metasedimentory rock with porphyritic granite and in the northern part contact between rhyolite and granite. The other associated ore minerals include wolframite, chalcopyrite, pyrite, stannite, pyrrhotite, cubanite, covellite etc. and EPMA studies confirm the presence of cassiterite, pyrite, chalcopyrite, pyrrhotite and sphalerite. The average concentration of ore reserves of Sn, W and Cu have been estimated at 2.23 million tonnes up to a depth of 237 m below MSL with average grade of 0.28% Sn, 0.18% W and 0.24% Cu (Wokhoo and Prasad, 1989) Ref. [29].

Fluid inclusion studies were carried out on the mineralized quartz veins associated with granite and rhyolite of Tosham igneous complex. The homogenization temperature (Th_{total}) of type-II (250 to 310 ℃) and type-III (158 to 245 ℃) and the estimated *P-T* condition of temperature was from type-III aqueous inclusions range from 310 to 460°C and pressure was from type-1A carbonic inclusions ranges from 2100 to 3500 bar (Fig. 7). The first ice melting temperature ranging from –50.0°C to –30.0°C suggest the presence of $FeCl_2/MgCl_2$ and more likely $CaCl_2$ in the fluid system. The lower the first

melting point suggests the possible presence of $NaCl+MgCl2± FeCl2$ in the brines or complicated mixtures of fluid salt is estimated. The salinity measured in the study area shows high to low salinity ranging from 1.9 wt.% to 42.68 wt.% NaCl eq. and form three clusters (high 37 to 42.68 wt.% NaCl eq. medium 15 to 22.98 wt.% NaCl eq. and low 1.2 wt.% to 10.46 wt.% NaCl eq.). This can also be seen in the plot of salinity vs. homogenisation temperature for the fluid inclusions (Fig. 8).

The fluids of type-IV were characterize by have very high salinity inclusions contain halite which is ranging from 37.5 to 39.45 wt.% NaCl equivalent are commonly found in the magmatic hydrothermal fluids (Bodner, 1995; Somani and Srivastva, 2000)) Ref. [30&31]. Keppler and Wyllie (1991) Ref. [32] states that if the orthomagmatic fluid was hypersaline, tin would have been strongly partitioning into the aqueous phase upon saturation of the granitic melt and early high temperature orthomagmatic tin mineralisation would have resulted. The high salinity magmatic fluid suggests orthomagmatic origin for tin is possible at Tosham.
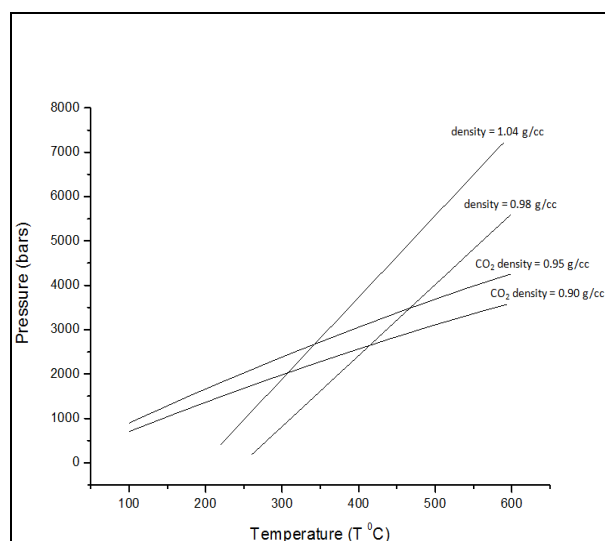

Figure 7. P–T estimation by the intersecting isochores of type-I (CO_2 inclusions density) and type-III (aqueous inclusions density) inclusions of mineralised quartz veins in Tosham area
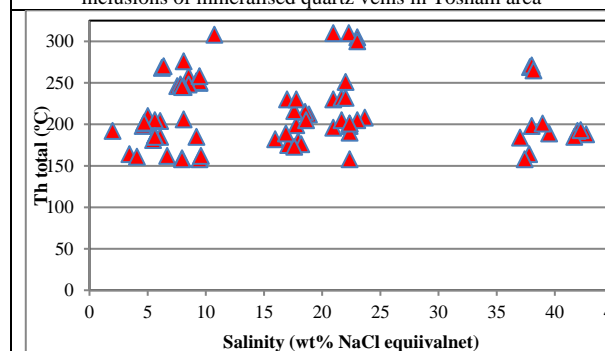

Figure 8. Salinity vs. Temperature of homogenisation (Th total) for the inclusions of mineralised quartz veins in Tosham area.

The second cluster having medium salinity ranging from 15 to 22.98 wt.% NaCl eq. are characterise by the aqueous carbonic phase (type-II) and aqueous phase (type-III) inclusions. These fluids characterised by the boiling

fluids after the formation of rhyolite explosion. This resulted, the rhyolite explosion breccias are formed and contain fragments of granite/quartzite and these fragments of granite porphyry are attributed to process of fluidisation. Higgins (1980) Ref. [33] suggested that the dissolved gas content of fluid plays an important role in promoting boiling and coupled to fluid rock reaction appears to have been the major cause of cassiterite precipitation at Tosham.

The type-II and type-III are homogenized in different ways, the inclusions show higher homogenisation temperatures and lesser salinities in type-II compare to type-III and numerous studies show that fluid mixing or fluid immiscibility are the dominant mechanisms for the precipitations of tin-tungsten complexes (Wang et al., 2012) Ref. [34]. Bowers and Helgeson show that a homogenous CO_2-H_2O-NaCl fluid can separate into immiscible CO_2 rich and H_2O rich fluids due to changes in either temperature or pressure. It is likely that immiscibility was caused initially by gradual cooling followed by a decrease in pressure. The phase separation of the fluids may have been induced by pressure fluctuation and it is evident that vapour rich and liquid rich inclusions are homogenised in the temperature ranges from 250 to 310°C and these temperatures represent the tin-tungsten mineralisation at Tosham.

A large no. CH_4 inclusions are dominated over the CO_2 inclusions and are reporting for the first time in this area and confirmed by Raman spectroscopy. The abundant CH4 fluid was considered to be one of the diagnostic features of reduced porphyry copper deposit environment (Zhang et. al., 2019) Ref. [35]. The last stage of fluid evolution the temperature (150 to 260°C) and low salinity (1.9 to 9.0 wt.% NaCl equivalent) indicating the mixing of the cooler meteoric waters with the hydrothermal solutions. The decline in salnity and temperature are also due to the loss of CO2 and this results deposition of sulphides.

Fluid inclusion studies reveal that ore fluids with high and low salinities in aqueous media with CO_2/CH_4 component and the presence of chlorides such as $FeCl_2$/$MgCl_2$ and $CaCl_2$ indicate the involvement of chlorine in transportation of Sn-W to the fluid system. The evaluation of ore forming fluids by high-salinity and high-temperature with the magmatic-hydrothermal activity either by immiscibility or mixing of fluids and evolution of granite/rhyolite induced the fluidisation and the presence of CH_4/CO_2 influx might have triggered precipitation Sn-W and copper mineralisation in the area.

CONFLICT OF INTEREST

The authors declare no conflict of interest.

ACKNOWLEDGMENT

AUTHOR CONTRIBUTIONS

Girish Kumar M, Manuscript written, Geological Field work, Analysed the samples in fluid inclusion studies and EPMA studies; Nevin, C. G., Geological Field work, Petrography, Analysed the samples in EPMA studies; Madhushree Mondal, Geological Field work, Ore petrography; Abhishek Anand, Geological Field work, Petrography; R.P. Nagar, Geological Field work, Supervision, discussion and correction of research paper; Subhaish Ghosh, Geological Field work, Supervision, discussion and correction of research paper; all authors had approved the final version.

REFERENCE

[1] C. A. McMahon, "Microscopic structures of Malani rocks of aravalli region," *Rec. Geol. Surv. India*, vol. 19, pp. 161–165, 1886.

[2] N. Kochhar, "Tosham ring complex, Bhivani India," in *Proc. Indian Nat Sci. Acad.*, vol. 49, no. 4, pp. 216–218, 1983.

[3] M, M. Rajashekharappa, "Petrographic studies and major elements data of all the rock types of the Tosham igneous complex, Tosham area, district Bhiwani, Haryana," Unpublished GSI FSP Report, 1983.

[4] S. C. Awasthi, M. Prasad, and V. K. Anand, "1981 Geology, structure and sulphide mineralization of Tosham," *Bhiwani District, Haryana. Rec. Geol. Surv*., p. 8, 1981.

[5] R. C. Dey, "Copper mineralization in tosham area, bhivani dist., haryana," *Indian Minerals*, pp. 27–32, 1978.

[6] A. K. Choudhary, K. Gopalan, and C. A. Sastry, "Present status of the geochronologyof Precambrian rocks of Rajasthan," *Tectonophysics*, vol. 105, pp. 131–140, 1984.

[7] N. Kochhar, "Rb-Sr age of the tosham ring complex, bhivani, India," *Jour. Geol. Soc. India*, vol. 26, pp. 216–218, 1985.

[8] R. L. Somani, "Evolution of tin-tungsten and copper bearing hydrothermal solutions associated with tosham igneous complex, tosham, bhiwani District, haryana: A fluid inclusion study," *Jour. Geol. Soc. India*, vol. 67, pp. 379–386, 2006.

[9] S. Murao, M. Deb, and M. Furuno, "Mineralogical evolution of indium in high grade tin-polymetallic hydrothermal veins – A comparative study from tosham, haryana, India and goka, naegi district, Japan," *Jour. Ore Geology Reviews*, vol. 33, pp. 490–504, 2008.

[10] B. Mishra and S. Srivastava, "Report on exploration for multi-metal prospect in north of tosham hill, bhiwani district, Haryana," GSI Unpublished Report, 2018.

[11] A. R. Campbell, C. J. Hackbarth, G. S. Plumlee, U. Petersen, "Internal features of ore minerals seen with the infrared microscope," *Econ. Geol.*, vol. 79, pp. 1387–1392, 1984.

[12] L. N. Gupta and M. M. Rajashekharappa, "Geology and mechanism of emplacement of ring dyke and associated rocks of the tosham igneous complex (haryana)," *Publ. Cent. Adv. Stud. Geol. Punjab Uni. Chandigarh*, vol. 13, pp. 250–273, 1983.

[13] R. K. Wakhloo and S. Prasad, "1989 Final report on phase I of Tosham tin investigation, bhiwani district, haryana, report," *Geol. Surv. Ind. F.S.*, 1982.

[14] J. L. Pouchou and F. Pichoir, "A new model for quantitative X-ray microanalysis," *Part I: Application to the Analysis of Homogeneous Samples: La Recherche Aerospatiale*, vol. 3, pp. 13–38, 1984.

[15] E. Roeder, "Fluid inclusions, reviews in mineralogy," *Min. Soc. America*, vol. 644, 1984.

[16] H. Z. Lu, H. R. Fan, P. Ni, G. X. Ou, K. Shen *et al.*, *Fluid Inclusions*, Science Press, Beijing, pp. 406–419, 2004.

[17] J. L. R.Touret, "Fluids in metamorphic rocks," *Lithos.*, vol. 55, pp. 1–25, 2001.

[18] R. J. Bodnar, P. R. Binns, and D. L. Hall, "Synthetic fluid inclusions – Quantitative evolution of the decrepitation behavior of fluid inclusions in quartz at one atmosphere confining pressure," *Jour. Met. Geol.*, vol. 7 pp. 229–242, 1989.

[19] R. J. Bakker, "Package fluids, computer programs for analysis of fluid inclusion data and modeling bulk fluid properties," *Chem. Geol.*, vol. 194, pp. 3–23, 2003.

[20] Y. G. Zhang and J. D. Frantz, "Determination of the homogenisation temperatures and densities of superficial fluids in the system NaCl-KCl-CaCl$_2$-H2O using synthetic fluids inclusions," *Chem. Geol.*, vol. 64, pp. 335–345, 1987.

[21] R. Bodnar, "Revised equation and table for determining the freezing point depression of H2O–NaCl solutions," *Geochim. Cosmochim. Acta*, vol. 57, p. 683, 1993.

[22] W. Duschek, R. Kleinrahm, and W. Wagner, "Measurement and correlation of the (pressure, density, temperature) relation of carbon dioxide, saturated-liquid and saturated-vapour density and the vapour pressure along the entire coexistence curve," *J. Chem. Thermodyn.*, vol. 22, pp. 841–864, 1990.

[23] U. Setzmann and W. Wagner, "A new equation of state and tables of thermodynamic properties for methane covering the range from the melting line to 625 K at pressures up to 1000 MPa," *J. Phys. Chem. Ref. Data*, vol. 20, pp. 1061–1155, 1991.

[24] R. Span and W. Wagner, "A new equation of state for carbon dioxide covering the fluid region from the triple- point temperature to 1100 K at pressures up to 800 MPa," *J. Phys. Chem. Ref. Data*, vol. 25, pp. 1509–1596, 1196.

[25] U. Setzmann and W. Wagner, "A new equation of state and tables of thermodynamic properties for methane covering the range from the melting line to 625 K at pressures up to 1000 MPa," *J. Phys. Chem. Ref. Data*, vol. 20, pp. 1061–1155, 1991.

[26] V. D. A. M. Kerkhof, "Phase transitions and molar volumes of CO$_2$–CH$_4$–N$_2$ inclusions," *Bulletin de Minéralogie*, vol. 111, pp. 257–266, 1988.

[27] P. E. Brown and W. M. Lamb, "P-V-T properties of fluids in the system H$_2$O-CO$_2$-NaCl: New graphical presentation and implications for fluid inclusion studies," *Geochim. Cosmochim. Acta*, vol. 53, pp. 1209-1221, 1988.

[28] T. J. Shepherd, A. H. Rankin, and D. H. M. Alderton, "A practical guide to fluid inclusion studies," *Blackie, Glasgow and London*, p. 239, 1985.

[29] R. K. Wakhloo and S. Prasad, "1989 Final report on phase I of Tosham tin investigation, bhiwani district,". *Surv. Ind.*, 1982.

[30] Bodnar, R. Fluid-inclusion evidence for a magmatic source for metals in porphyry copper deposits. In: Thompson, J.F.H. Ed., Magmas, Fluids, and Ore Deposits. Mineralogical Association of Canada Short Course, Victoria, British Columbia, pp. 139–152, 1995.

[31] R. L. Somani and P. K. Srivastava, "Origin and evolution of hydrothermal fluids associated with granitoid-host-edtungsten mineralization at Degana," *Jour. Geol. Soc. India*, vol. 56, pp. 661–671, 2000.

[32] H. Keppler, P. J. Wyllie, "Partitioning of Cu, Sn, Mo, W, U, and Th between melt and aqueous fluid in the systems haplogranite– H/O–HCl and haplogranite–H20–HF," *Contributions to Mineralogy and Petrology*, vol. 109, pp. 139–150, 1991.

[33] Higgins, "Fluid inclusion evidence for the transport of tungsten by carbonate complexes in hydrothermal solutions," *Canadian Journal Earth Science*, vol. 17, pp. 823–830, 1980.

[34] X. D. Wang *et al.,* "Fluid inclusion studies of the Huangsha quartz– vein type tungsten deposit," *Acta Petrol. Sinica*, vol. 28. pp. 122–132, 2012.

[35] Z. Wei *et al.*, "The origin of CH4-rich fluids in reduced porphyry –Skarn Cu–Mo–Au systems," *Jour of Ore Geology*, vol. 114 ,pp. 103–135, 2019.